
AneuG-Flow: A Large-Scale Synthetic Dataset of Diverse Intracranial Aneurysm Geometries and Hemodynamics

Wenhai Ding

Department of Biomedical Engineering
Imperial College London
United Kingdom
w.ding23@imperial.ac.uk

Yiying Sheng*

Department of Biomedical Engineering
National University of Singapore
Singapore
yiyings@nus.edu.sg

Simão Castro

Department of Mechanical Engineering
Instituto Superior Técnico
Portugal
simao.vitoriano@tecnico.ulisboa.pt

Hwa Liang Leo

Department of Biomedical Engineering
National University of Singapore
Singapore
bielhl@nus.edu.sg

Choon Hwai Yap

Department of Biomedical Engineering
Imperial College London
United Kingdom
c.yap@imperial.ac.uk

Abstract

1 Hemodynamics has a substantial influence on normal cardiovascular growth and
2 disease formation, but requires time-consuming simulations to obtain. Deep Learn-
3 ing algorithms to rapidly predict hemodynamics parameters can be very useful,
4 but their development is hindered by the lack of large dataset on anatomic ge-
5ometries and associated fluid dynamics. This paper presents a new large-scale
6 dataset of intracranial aneurysm (IA) geometries and hemodynamics to support
7 the development of neural operators to solve geometry-dependent flow governing
8 partial differential equations. The dataset includes 14,000 steady-flow cases and
9 570 pulsatile-flow cases simulated with computational fluid dynamics. All cases
10 are computed using a laminar flow setup with more than 3 million cells. Boundary
11 conditions are defined as a parabolic velocity profile with a realistic waveform
12 over time at the inlet, and geometry-dependent mass flow split ratios at the two
13 downstream outlets. The geometries are generated by a deep generative model
14 trained on a cohort of 109 real IAs located at the middle cerebral artery bifurcation,
15 capturing a wide range of geometric variations in both aneurysm sacs and parent
16 vessels. Simulation results shows substantial influence of geometry on fluid forces
17 and flow patterns. In addition to surface mesh files, the dataset provides volume
18 data of velocity, pressure, and wall shear stresses (WSS). For transient cases, spatial
19 and temporal gradients of velocity and pressure are also included. The dataset is
20 tested with PointNet and graph U-Nets for WSS prediction, which showed relative
21 L2 loss of 4.67% for normalized WSS pattern.

*The first and second authors contributed equally to this work.

22 **1 Introduction**

23 For many vascular diseases, there has been a long history of investigating fluid mechanics behaviors
24 aimed at improving surgical decision-making and post-operative treatment [1]. However, a significant
25 gap remains between biomechanics research and its adoption in clinical practice. A clear example of
26 this gap is intracranial aneurysm (IA)—a condition where a weakness in the vessel wall leads to a
27 bulge that carries a potentially lethal risk of rupture [2]. Despite extensive research in biomechanics
28 and several meta studies suggesting a correlation between biomechanical markers and aneurysm
29 instability [3], these markers have yet to be accepted or utilized by physicians. In practice, physicians
30 continue to rely primarily on morphological markers [4] to assess rupture risk, even though such
31 systems [5] have been reported to suffer from high false-positive rates (up to 56%) [6].

32 One of the key reasons for this gap is that fluid dynamics simulations are time-consuming and require
33 specialized expertise. As a result, physicians are unable to obtain fluid dynamics data in sufficiently
34 large sample sizes to evaluate the clinical utility of biomechanics markers, preventing their adoption
35 of it. As such, it would be useful to develop deep learning models for rapid prediction of flow
36 dynamics in disease morphologies. Driven by this clinical demand, the concept of predicting CFD
37 solutions directly from vascular geometries has gained significant momentum in recent years. In
38 terms of application domains, models have been developed for coronary arteries [7], aorta [8], aortic
39 aneurysms [9], and the left ventricle [10]. From a methodological perspective, both supervised and
40 self-supervised models are actively being explored. Representative work in the supervised category
41 includes a family of geometry-informed neural operators [10, 11, 12, 13], while self-supervised
42 approaches—such as [14, 15, 16]—leverage physics-informed training. Both approaches require a
43 substantial dataset for training and/or validation.

44 Unfortunately, available datasets in the bioengineering domain to support such tasks are far from sat-
45 isfactory. Most existing studies—particularly those focused on theoretical model development—rely
46 on idealized geometry datasets. For instance, simple harmonic functions are employed in [15] and
47 [16] to represent the 3D geometries of coronary arteries. Similarly, models in the geometry-informed
48 neural operator family are often evaluated on highly simplified and impractical geometric domains
49 [11], limiting their translational relevance to real-world applications. This limitation largely stems
50 from the inherent difficulty of assembling a sufficient range of patient-specific geometries. As shown
51 in Table 1, most available datasets contain only a few hundred geometries. Moreover, generating the
52 corresponding CFD solutions demands significant High-Performance Computing (HPC) resources
53 and considerable human expertise to design, tune, and maintain an efficient simulation workflow.

54 In addition to being limited in scale, several existing datasets suffer from other notable shortcomings.
55 For example, [17] provides real aneurysm sac geometries, but attaches them to a single idealized
56 mother vessel, resulting in globally unphysiological vascular structures with no variation. Similarly,
57 while [18] offers a large-scale dataset, over 95% of them are manually deformed from real shapes
58 rather than being generated through data-driven approaches, and the parent vessels were not generated
59 even though they are critical to flow behaviors. To address the shortage of realistic 3D hemodynamics
60 data and to offer a more physiological and large-scale alternative, we introduce a new dataset of IA
61 geometries with associated hemodynamics. The main contributions are summarized as follows:

- 62 • We provide the first large hemodynamics dataset of both IA 3D geometry and its detailed
63 hemodynamics where both aneurysm pouch and parent vessels are modelled. Geometries
64 show decent diversity representative of that of clinical data.
- 65 • A relatively large amount of geometries are provided compared to existing datasets in the
66 bioengineering community. We include 14,000 steady cases and 200 pulsatile cases.
- 67 • In addition to the volume data, we provide wall shear stress (WSS) solution on IA sac
68 surfaces with a consistent mesh graph structure (connectivity), allowing easier downstream
69 deep learning processing.

70 **2 Case Description**

71 **2.1 Geometry**

72 Unlike existing datasets which create geometry variations by manually warping real shapes [9, 18],
73 we use a generative model AneuG [19] that learns the geometry distribution from a real IA cohort.

Table 1: Review on hemodynamics datasets

Dataset	Anatomical region	Size	Geometry source
[9]	Aortic aneurysm	230	Manually generated from 23 real shapes.
AnXplore[17]	Intracranial aneurysm	101	Real IA sac geometries merged with the same idealized mother vessel.
Aneumo[18]	Intracranial aneurysm	10,000	9,534 synthetic shapes manually generated from 466 real shapes.
AneuG-Flow (Ours)	Intracranial aneurysm (with parent vessels)	14,000	Synthetic shapes generated with a generative model trained on a cohort of 116 real shapes.

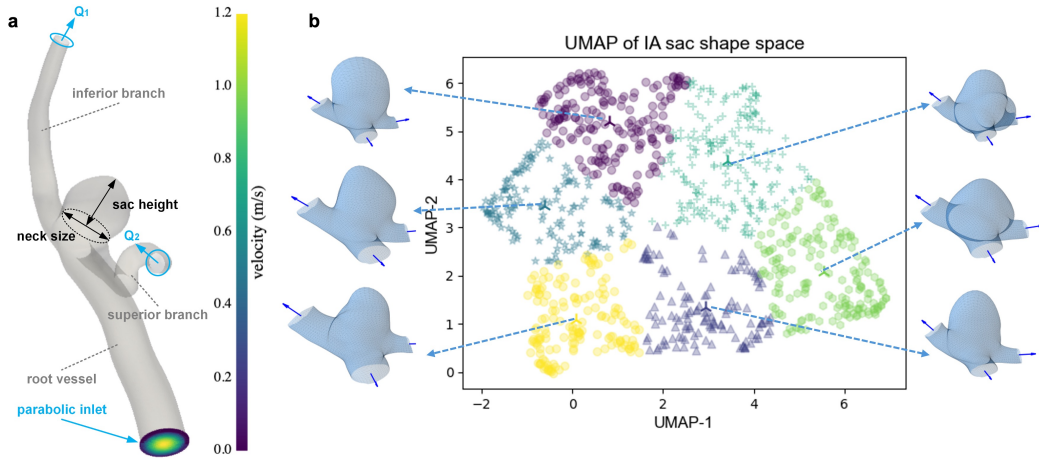


Figure 1: Geometry configuration. a: Flow configuration. b: UMAP of aneurysm sac geometries.

74 AneuG leverages the technique of Graph Harmonic Deform (GHD) [20] to encode the spatial warping
 75 of real IA shapes with respect to a canonical shape into a sequence of tokens. The distribution of
 76 tokens are then approximated with a two-stage Variational Autoencoder (VAE). More details can
 77 be found in [19] and [20]. AneuG generates both the aneurysm sac and its parent vessels, with the
 78 latter being conditioned on the former. This approach allows us to create diverse physiological IA
 79 shapes for CFD simulations, while existing works such as [17] fails to capture the joint distribution
 80 of aneurysm sacs and their parent vessels. AneuG uses data from the AneuX morphology database
 81 [21], an open-access, multi-centric database combining data from three European projects: AneuX
 82 project, @neurIST project and Aneurisk. As reported in [21], all patients/participants provided
 83 written informed consent to participate in the study.

84 As shown in Fig. 1, we create IAs located at the bifurcation of the middle cerebral artery (MCA).
 85 Such a topology contains one root vessel and two downstream vessel branches (referred to as the
 86 inferior and superior branch). Compared to the inferior branch, the superior branch generally has
 87 smaller radius and larger spatial angle with respect to the root vessel.

88 2.2 Mesh Generation Pipeline

89 We assembled a set of open-source repositories and commercial software automation scripts to
 90 develop a fully automated pipeline for volume mesh generation. Low-resolution surface meshes
 91 generated from AneuG were processed using Geomagic Wrap v2024.3.0 for remeshing and localized
 92 smoothing. We then used the Vascular Modeling Toolkit (VMTK) to generate 3D volume meshes
 93 (codes modified from [8]). For each case, 4 inflation layers were applied with a total thickness
 94 equal to 0.5 times the local edge length near the wall. The final meshes contained an average of 3.4
 95 million volume cells, which mesh convergence studies have shown to be sufficient (see supplementary

96 materials for details). This pipeline is generalizable to vascular structures with a fixed number of
97 inlets and outlets. We provide the codes at [22].

98 **2.3 Boundary Conditions**

99 As shown in Fig. 1, we apply a parabolic velocity profile at the inlet with an average velocity
100 of 0.684 m/s, as measured in [23]. For the outlets, several studies have demonstrated that flow
101 split conditions more accurately represent physiological hemodynamics compared to fixed pressure
102 boundaries [24, 25]. Following these work, we determine the mass flow split between the superior
103 and inferior branches using a modified form of Murray’s law:

$$\frac{Q_1}{Q_2} = \left(\frac{D_1}{D_2} \right)^\gamma \quad (1)$$

104 where Q_1 and Q_2 are the outlet flow rates, D_1 and D_2 are the corresponding vessel diameters, and γ
105 is the flow split exponent. We follow [26] and choose $\gamma = 2.45$. This formulation ensures that the
106 outlet boundary conditions reflect geometry-dependent mass flow split.

107 Blood were assumed as imcompressible non-Newtonian fluid. We adopt the Carreau–Yasuda model
108 to account for the non-Newtonian behavior of blood:

$$\mu(\dot{\gamma}) = \mu_\infty + (\mu_0 - \mu_\infty) [1 + (\lambda\dot{\gamma})^a]^{\frac{n-1}{a}} \quad (2)$$

109 The model parameters are set as follows: zero-shear viscosity $\mu_0 = 0.056$ Pa·s, infinite-shear
110 viscosity $\mu_\infty = 0.00345$ Pa·s, time constant $\lambda = 3.313$ s, and power-law index $n = 0.3568$. The
111 Yasuda parameter is assumed to be $a = 2$ and the blood density is set to 1050 kg/m³.

112 An laminar flow setup was used, as the average Reynolds numbers in the root vessel and downstream
113 branches were approximately 410 and 330, respectively. And vessel walls were assumed as rigid
114 with a no-slip condition. Since measurements of blood pressure and flow velocity are not routinely
115 performed during the clinical management of intracranial aneurysms, an average waveform reported
116 in [27] was adopted for all transient simulations. The average inlet velocity was kept same across all
117 morphologies to ensure that aneurysms with larger parent vessels experienced higher mass flow rates.
118 The velocity waveform signal is included in our dataset. Each transient case was simulated over two
119 cardiac cycles using a time step of 0.001, s, which was confirmed to be sufficient through a time-step
120 convergence study. Only the results from the second cycle were extracted.

121 **2.4 Solver and HPC Setup**

122 All simulations were performed using ANSYS Fluent 2023R2 (ANSYS Inc., Canonsburg, PA, USA)
123 on the High-Performance Computing (HPC) Services at Imperial College London and National
124 University of Singapore. Simulations ran on AMD nodes, each contains 128 cores and 1TB RAM.
125 The Research Data Store at Imperial College London were used for data storage during the runs.
126 Each simulation was run on a single AMD node using 64 cores. Each case took approximately 3
127 minutes to mesh, and 2 minutes to solve the steady simulation. Transient cases each took around 10
128 hours to solve.

129 **2.5 Graph structural consistency during CFD data extraction**

130 In addition to the raw CFD solution data, we also provide additional post-processed WSS on
131 the surfaces of IA sacs as graphs. Each graph contains the same number of nodes and the same
132 connectivity, allowing easier implementation of downstream deep learning tasks. AneuG generates
133 surface meshes using a mesh morphing approach, where every case has exactly 3500 triangle faces for
134 the aneurysm sac [19]. As this mesh size is of low resolution, we subdivided each triangular element
135 by adding a new node at the center of the each edge and dividing the element into four new elements,
136 leading to 14,000 faces. WSS at nodes were then extracted through k-NN interpolation method from
137 [23]. Further subdivision can be performed if higher resolution is desired. The standardization of node
138 and connectivity structure allows a natural and easy node-to-node / edge-to-edge registration between
139 different IA cases, and facilitates deep learning processing. The associated graph connectivity is also
140 provided (see Table 2). Extraction codes are available at [22].

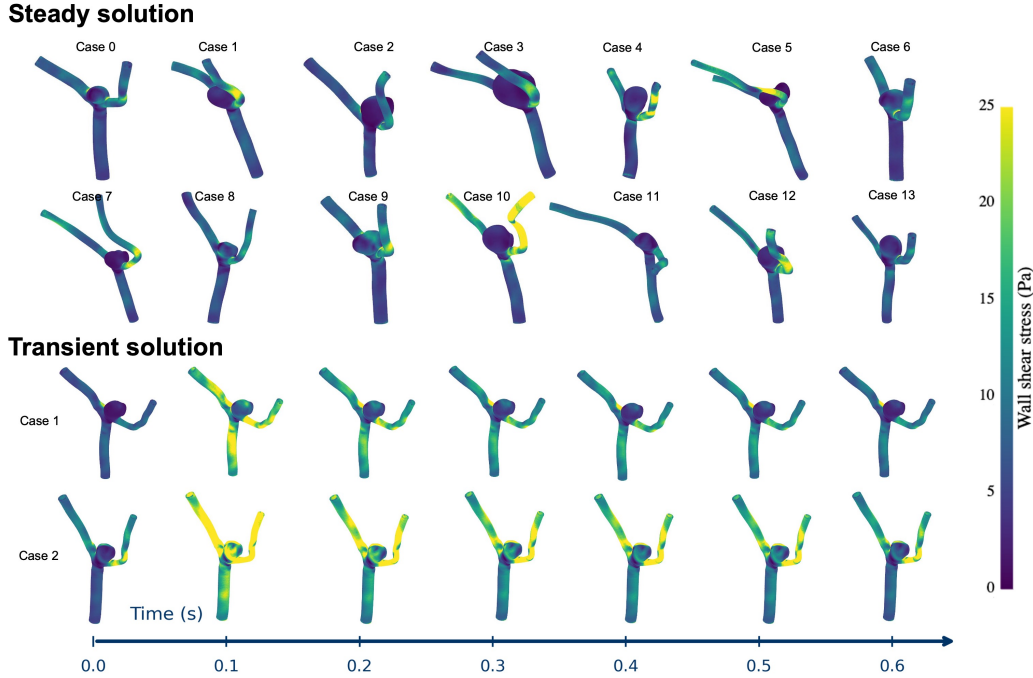


Figure 2: Example of wall shear stress data.

141 3 Dataset Description

142 3.1 Geometry Variation

143 We follow [19] to generate synthetic shapes using pretrained checkpoint files. Latent features were
 144 sampled from a 64-dimensional uniform distribution with a mean of 0 and a standard deviation of
 145 2.5, and were subsequently passed through the decoder. We chose this setup because it covers over
 146 98% of the latent space of a theoretically well-trained VAE. It is also the maximum deviation from
 147 the latent space center that still yields physiologically plausible shapes. As shown in Fig. 1 b, diverse
 148 aneurysm sac geometries are included.

149 3.2 Dataset Contents

150 A summary of the content of this dataset is provided in Table 2 and Table 3. For steady cases, we
 151 assemble the solution data of all cases into one Pytorch .pth file while keeping geometry-dependent
 152 files in separate case folders. As mentioned above, we also provide node-to-node registration for the
 153 aneurysm sac region to construct a well-structured PyTorch tensor object. This tensor has the shape
 154 of $[B, N, C]$, where B , N , and C denote the number of cases, the number of surface nodes, and the
 155 number of physics variables, respectively.

156 We also provide a list of downsampled node indexes and associated edge connection of downsampled
 157 meshes obtained using the method described in [29]. This downsampling approach preserves the
 158 topological integrity of the shapes, whereas generating low-resolution k-NN graphs based solely on
 159 Euclidean coordinates may introduce connections between points that are close in space but distant
 160 in terms of surface geodesic distance. These graph structures can be used for U-Net-like structures
 161 with graph convolution layers. A visualization is provided in Fig. 3

162 For transient cases, we provide time-series data over one full cardiac cycle, as summarized in Table 3.
 163 Solutions were extracted at 80 uniformly spaced time steps within the second cardiac cycle, resulting
 164 in each PyTorch tensor object having the shape $[T, N, 1]$, where T denotes the number of time steps
 165 and N the number of nodes. PyTorch .pth files were saved separately within each case folder.

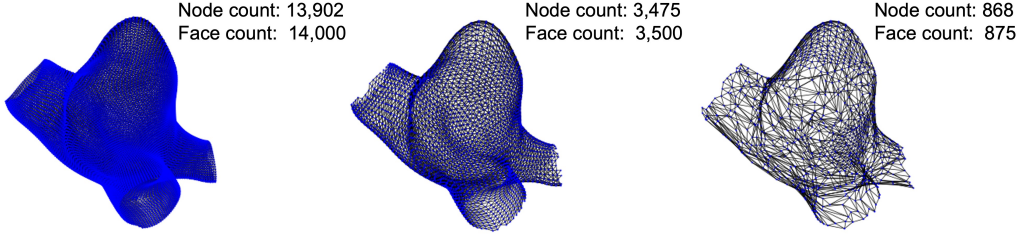


Figure 3: Mesh downsampling.

Table 2: Dataset contents of steady cases

Solution data		
File & Structure	Keys	Content
Raw_data.pth List[Dict[str, Any]]	label	List of solution variable names.
	tensor	PyTorch tensor object of solution data.
	ghd	GHD tokens [19] and rigid alignment checkpoints.
	log	Fluent residuals log.
	case_name	Case name.
Registered_data.pth Dict[str, Any]	tensor	PyTorch tensor object of registered solution data.
	tensor_norm	Mean and standard deviation of registered data.
	idx_list	Vertex index list of downsampled surface meshes.
	edge_index_list	Edge connections of downsampled surface meshes.
	ds_factors	List of downsampling factors.
Geometry data (inside each case folder)		
	flowsplit_ratio.txt	Mass flow split ratio between two outlets.
	shape.obj	Surface mesh generated by AneuG.
	shape_remeshed.obj	Post-processed surface mesh (by Geomagic).

166 3.3 How to access the dataset

167 The **AneuG-Flow** dataset is open-source under a CC BY-SA 4.0 license. It can be accessed and
168 downloaded directly from the Hugging Face Hub. Codes are available at [22].

169 3.4 Limitations

170 We aim to provide a large-scale hemodynamics dataset to support the prediction of biomechanical
171 markers directly from patient-specific vascular geometries. However, several limitations remain. First,
172 the dataset includes a relatively small number of transient cases (578) compared to that of steady
173 cases (14,000), which may limit its utility for predicting temporal biomechanical markers such as
174 time-averaged wall shear stress and oscillatory shear index. Expanding the dataset with more transient
175 simulations is a priority for our future work. Second, the current dataset is limited to geometries with
176 a single inlet and two outlets. To improve generalizability, additional vascular topologies — such as
177 shapes with a single inlet and a single outlet — should be incorporated in the next phase. Finally, we
178 do not consider variations of boundary conditions at the moment, as measuring blood pressure and
179 mass flow waveform signals in the middle cerebral artery is not yet a routine in clinical practice.

Table 3: Dataset contents of transient cases

Solution data (inside each case folder)		
File & Structure	Keys	Content
blood_data.pt Dict[str, Tensor]	various	Volume solution data of the blood domain, including spatial coordinates, velocity components, pressure, viscosity, temporal derivative of pressure, and spatial derivatives of velocity components.
wall_data.pt Dict[str, Tensor]	various	solution data of the surface domain, including spatial coordinates, Wall shear stress components, and the total wall shear stress magnitude.
Geometry data (inside each case folder)		
same as Table 2		

180 4 ML Evaluation

181 We demonstrate a simple regression task as an application of the dataset. Given the geometries of
 182 IAs, we train several baseline models to predict the steady-state WSS map on the aneurysm sac.
 183 Leveraging the surface node-to-node registration described in Section 2.5, we construct input graphs
 184 with the same connectivity across different cases, each containing 13,902 nodes and 14,000 triangles.
 185 The network is designed to output WSS vector components in the x , y , and z directions. We use 80%
 186 of the steady-state cases for training and the remaining 20% for testing.

187 **Networks & loss function design.** We adopt a U-Net-like structures for the models. Specifically,
 188 we train a PointNet++ and three graph U-Nets: one using simple Graph Convolutional Networks
 189 (GCN), another using Graph Attention Networks (GAT), and a third using Chebyshev Spectral Graph
 190 Networks (ChebNet) as the core convolutional layers. For PointNet++, downsampling is performed
 191 using farthest point sampling (FPS) [28]. For graph U-Nets, a pre-computed set of downsampled
 192 node indices and associated edge connections was used, as mentioned in Section 3.2. A visualization
 193 of the mesh downsampling is provided in Fig. 3. In addition to the mean squared error (MSE) loss
 194 computed on z-score-normalized wall shear stress (WSS), we also evaluate an MSE loss defined on
 195 WSS values normalized using an power mapping:

$$\mathcal{L}_{\text{exp}} = \text{MSE} [f(w^{\text{pred}}), f(w^{\text{true}})], \quad f(w) = \left(\frac{\alpha \cdot w}{w_{\max}} \right)^{\beta} \cdot \frac{1}{\alpha} \quad (3)$$

196 where w denotes the WSS components and f is the normalization function. α and β are manually
 197 selected hyperparameters. For this task, we chose $\alpha = 100$ and $\beta = \frac{2}{3}$. We introduce this loss term
 198 because high WSS values often appear near the junction areas between the aneurysm sac and its
 199 parent vessels. However, it is the low WSS distribution on the sac that is generally considered more
 200 clinically significant by physicians [3]. By applying such a nonlinear normalization to the WSS,
 201 the model is encouraged to learn the overall spatial pattern of WSS rather than being dominated by
 202 high-magnitude areas. As shown in Fig. 4, the normalized WSS exhibits reduced contrast between
 203 high and low values, thereby emphasizing the underlying distribution pattern.

204 **Metrics & Results.** Each model is trained on a single NVIDIA RTX 3090 GPU for 24 hours, with
 205 the learning rate decayed by a factor of 0.75 every 100 epochs. Model performance is evaluated
 206 using the root mean square error (RMSE) and mean absolute error (MAE) computed on the WSS
 207 values. In addition, both metrics and the relative L2 error are computed on WSS normalized using
 208 Eq. (3), which reflects the model’s capability of predicting the spatial pattern of WSS. Prediction
 209 performances are visualized for three random cases in Fig. 4. The model captures the global WSS
 210 map on the aneurysm sac well. As expected, high WSS is observed near the junction between the sac
 211 and the parent vessels, while low WSS appears around lobulated regions on the sac. Among different
 212 network designs, the U-Net using ChebNet as the convolutional layer performs the best. During
 213 training, the ChebNet kernel size was set to 3, and all networks were configured with identical depth

Table 4: Model performance evaluated on WSS and Eq. (3)-normalized WSS.

Model	WSS		Normalized WSS		
	RMSE (Pa)	MAE (Pa)	RMSE	MAE	Relative L2 (%)
PointNet++	0.204	0.122	0.0353	0.0263	5.39
U-Net (GCN)	0.199	0.114	0.0317	0.0233	4.82
U-Net (GAT)	0.213	0.120	0.0333	0.0242	5.04
U-Net (ChebNet)	0.191	0.108	0.0307	0.0223	4.67

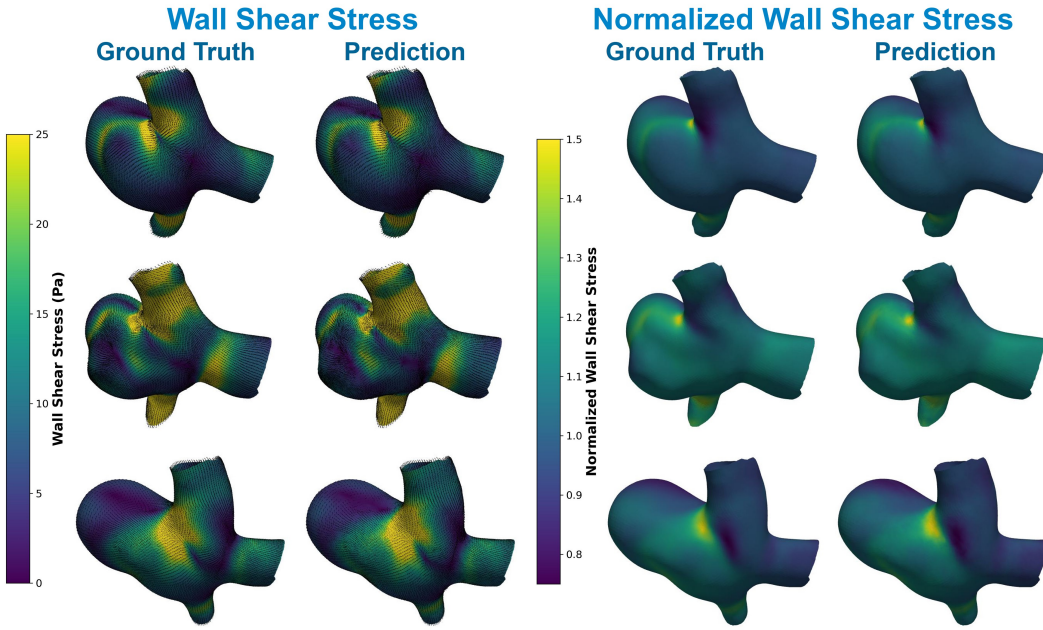


Figure 4: Prediction of WSS and WSS normalized with Eq. (3) from the trained U-Net (GCN).

214 and channel dimensions. The better performance is likely attributable to the enhanced receptive field
215 of ChebNet, allowing more effective propagation of information across the mesh.

216 5 Relationship between morphological & biomechanical markers

217 We go beyond steady cases and investigate the relationship between morphological markers and
218 biomechanical markers on our transient data. For morphological markers, we include Aspect Ratio
219 (AR), Size Ratio (SR), and maximum sac height (H_{max}) as they are generally accepted in existing
220 physiology research [4, 5]. Further, We include Lobulation Index (LI) defined as the sac's surface
221 area divided by its volume. We also compute the radius of a sphere with the same volume of the sac
222 as it reflects the 3D size of the aneurysm, which we refer to as Equivalent Radius (ER). A detailed
223 graphic definition of these markers can be found in the supplementary material. For biomechanical
224 markers, we consider two of them: Oscillatory Shear Index (OSI) and Relative Residence Time
225 (RRT) [30]. The Oscillatory Shear Index (OSI) measures the directional changes of wall shear stress
226 throughout a cardiac cycle, defined as:

$$227 \text{OSI} = \frac{1}{2} \times \left(1 - \frac{\left| \int_0^T \tau_w(t) dt \right|}{\int_0^T |\tau_w(t)| dt} \right) \quad (4)$$

228 with values ranging from 0 (unidirectional flow) to 0.5 (oscillatory flow). Relative Residence Time
(RRT) combines both parameters to evaluate flow stagnation:

$$RRT = \frac{1}{(1 - 2 \times OSI) \times TAWSS} \quad (5)$$

where Time-Averaged Wall Shear Stress (TAWSS) is the average magnitude of wall shear stress over a complete cardiac cycle, calculated as:

$$TAWSS = \frac{1}{T} \int_0^T |\tau_w(t)| dt \quad (6)$$

It is generally considered dangerous when large OSI and RRT are observed on the aneurysm sac's surface. As shown in Fig. 5 and Fig. 6, most morphological markers demonstrated weak or statistically insignificant correlations with both OSI and RRT averaged on the aneurysm sac. This suggests that traditional morphological markers alone may be insufficient to capture the complex hemodynamic behavior within aneurysmal sacs.

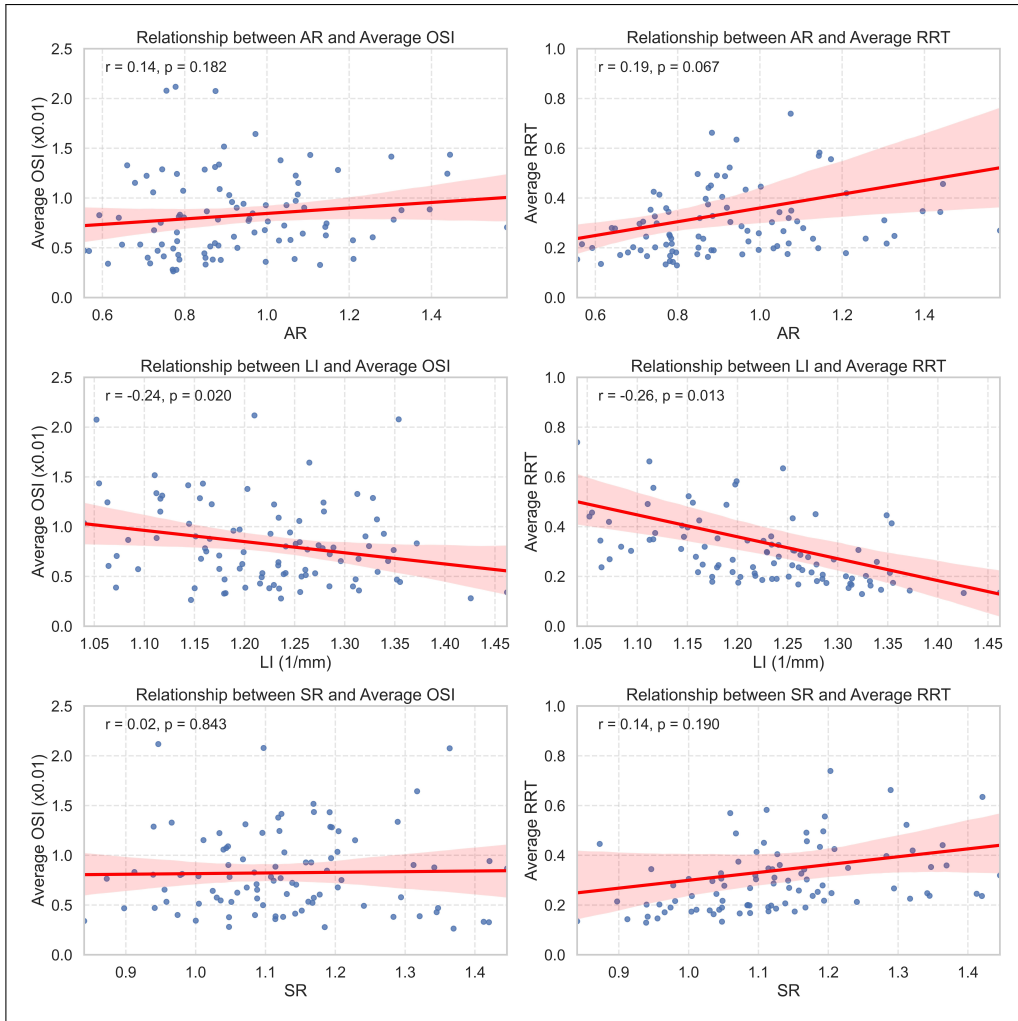


Figure 5: Morphological–biomechanical marker correlations (AR, SR, LI).

An interesting observation is the moderate but statistically significant negative correlation between the lobulation index (LI) and both OSI ($r = -0.24, p = 0.020$) and RRT ($r = -0.26, p = 0.013$). While this trend is statistically supported, it is counterintuitive. One would expect aneurysms with higher LI to be associated with more chaotic and oscillatory flow patterns. A possible explanation is that true daughter sacs—often linked to rupture risk and flow complexity—were relatively rare. And

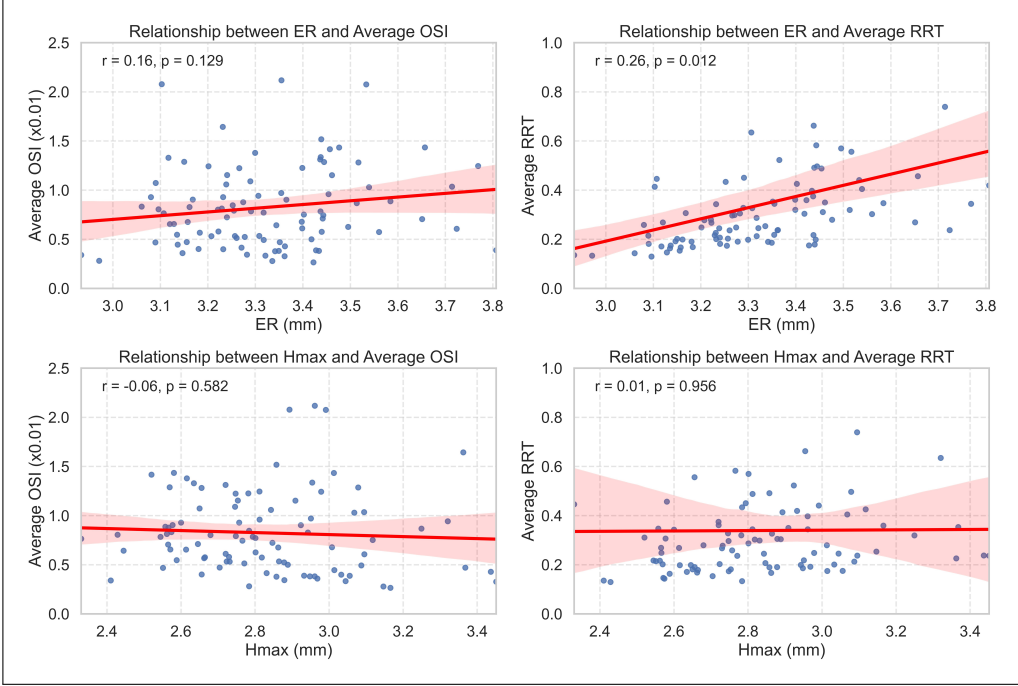


Figure 6: Morphological–biomechanical marker correlations (ER and H_{max})

241 the LI marker as defined here, may be elevated in aneurysms with elongated but smooth morphologies.
 242 These cases could exhibit high surface-to-volume ratios without necessarily possessing complex
 243 internal flow structures. Therefore, the specificity of LI as a marker may be limited. In contrast, the
 244 equivalent radius (ER), which reflects the size of the aneurysm sac based on its volume, showed a
 245 moderate positive correlation with both OSI ($r = 0.16, p = 0.129$) and RRT ($r = 0.26, p = 0.012$).
 246 This trend is intuitive, as a larger ER corresponds to a larger sac volume, increasing the likelihood
 247 of developing slow and recirculating flow. Such regions are typically associated with disturbed
 248 hemodynamics behaviors, including elevated oscillatory shear and prolonged residence time.

249 6 Conclusion

250 In this paper, we present a new large-scale and open-source dataset designed to support the devel-
 251 opment of data-driven models for predicting hemodynamics from geometries. The dataset includes
 252 14,000 steady-flow cases and 200 pulsatile-flow cases, each computed using high-resolution CFD sim-
 253 ulations with anatomically physiological IA geometries. These geometries model both the aneurysm
 254 sacs and their parent vessels as a joint distribution, addressing key limitations in previous datasets
 255 that relied on idealized or manually deformed shapes [9, 18].

256 By leveraging a deep generative model trained on a real IA cohort, we capture a broad range of
 257 physiologically plausible geometries representative of real-world anatomical variations. We provide
 258 solution data including pressure, velocity, and WSS. Spatial gradients for velocity components and
 259 temporal gradient for pressure are also provided. Initial experiments using PointNet and graph U-Nets
 260 demonstrate the dataset’s utility in enabling WSS pattern prediction, achieving a best relative L2 error
 261 of 4.67% on normalized WSS.

262 We hope this dataset will contribute to the biomechanics and machine learning communities, acceler-
 263 ating the development of neural operators and other data-driven solvers for geometry-conditioned
 264 partial differential equations.

265 **References**

- 266 [1] Carpenter, H.J., Gholipour, A., Ghayesh, M.H., Zander, A.C., Psaltis, P.J.: A review on the
267 biomechanics of coronary arteries. International Journal of Engineering Science **147**, 103201
268 (2020).
- 269 [2] Lee, K.S., Zhang, J.J.Y., Nguyen, V., Han, J., Johnson, J.N., Kirollos, R., Teo, M.: The Evolution
270 of Intracranial Aneurysm Treatment Techniques and Future Directions. Neurosurgical Review
271 **45**(1), 1–25 (2022).
- 272 [3] Zhou, G., Zhu, Y., Yin, Y., Su, M., Li, M.: Association of Wall Shear Stress with Intracranial
273 Aneurysm Rupture: Systematic Review and Meta-Analysis. Scientific Reports **7**(1), 5331
274 (2017).
- 275 [4] Merritt, W.C., Berns, H.F., Ducruet, A.F., Becker, T.A.: Definitions of intracranial aneurysm
276 size and morphology: A call for standardization. Surgical Neurology International **12**, 506
277 (2021).
- 278 [5] Etminan, N., Brown, R.D., Jr., Beseoglu, K., et al.: The Unruptured Intracranial Aneurysm
279 Treatment Score: A Multidisciplinary Consensus. Neurology **85**(10), 881–889 (2015).
- 280 [6] Mocco, J., Brown, R.D., Torner, J.C., Capuano, A.W., Fargen, K.M., Raghavan, M.L., Piepras,
281 D.G., Meissner, I., Huston, J.: Aneurysm Morphology and Prediction of Rupture: An Interna-
282 tional Study of Unruptured Intracranial Aneurysms Analysis. Neurosurgery **82**(4), 491–496
283 (2018).
- 284 [7] Li, G., Wang, H., Zhang, M. et al.: Prediction of 3D Cardiovascular Hemodynamics Before
285 and After Coronary Artery Bypass Surgery via Deep Learning. Communications Biology **4**, 99
286 (2021).
- 287 [8] Pajaziti, E., Montalt-Tordera, J., Capelli, C., Sivera, R., Sauvage, E., Quail, M., Schievano,
288 S., Muthurangu, V.: Shape-Driven Deep Neural Networks for Fast Acquisition of Aortic 3D
289 Pressure and Velocity Flow Fields. PLOS Computational Biology **19**(4), e1011055 (2023). doi:
290 10.1371/journal.pcbi.1011055.
- 291 [9] Faisal, M.A.A., Mutlu, O., Mahmud, S. et al.: Rapid Wall Shear Stress Prediction for Aortic
292 Aneurysms Using Deep Learning: A Fast Alternative to CFD. Medical & Biological Engineering
293 & Computing (2025).
- 294 [10] Yin, M., Charon, N., Brody, R. et al.: A Scalable Framework for Learning the Geometry-
295 Dependent Solution Operators of Partial Differential Equations. Nature Computational Science
296 **4**, 928–940 (2024).
- 297 [11] Li, Z., Huang, D.Z., Liu, B., Anandkumar, A.: Fourier Neural Operator with Learned Deforma-
298 tions for PDEs on General Geometries. Journal of Machine Learning Research **24**(1), Article
299 No. 388, 18593–18618 (2023).
- 300 [12] Quackenbush, B., Atzberger, P.J.: Transferable Foundation Models for Geometric Tasks on
301 Point Cloud Representations: Geometric Neural Operators. arXiv preprint arXiv:2503.04649
302 (2025).
- 303 [13] Quackenbush, B., Atzberger, P.J.: Geometric Neural Operators (GNPs) for Data-Driven Deep
304 Learning of Non-Euclidean Operators. arXiv preprint arXiv:2404.10843 (2024).
- 305 [14] Zhong, W., Meidani, H.: Physics-Informed Geometry-Aware Neural Operator. Computer
306 Methods in Applied Mechanics and Engineering **434**, 117540 (2025).
- 307 [15] Wong, H.S., Chan, W.X., Li, B.H. et al.: Strategies for Multi-Case Physics-Informed Neural
308 Networks for Tube Flows: A Study Using 2D Flow Scenarios. Scientific Reports **14**, 11577
309 (2024).
- 310 [16] Chan, W.X., Ding, W., Li, B., Wong, H.S., Yap, C.H.: Role of Physics-Informed Constraints
311 in Real-Time Estimation of 3D Vascular Fluid Dynamics Using Multi-Case Neural Network.
312 Computers in Biology and Medicine **190**, 110074 (2025).
- 313 [17] Goetz, A., Jeken-Rico, P., Pelissier, U., Chau, Y., Sédat, J., Hachem, E.: AnXplore: a comprehen-
314 sive fluid-structure interaction study of 101 intracranial aneurysms. Frontiers in Bioengineering
315 and Biotechnology **12** (2024).

- 316 [18] Li, X., Zhou, Y., Xiao, F., Guo, X., Zhang, Y., Jiang, C., Ge, J., Wang, X., Wang, Q., Zhang,
 317 T., Lin, C., Cheng, Y., Qi, Y.: Aneumo: A Large-Scale Comprehensive Synthetic Dataset of
 318 Aneurysm Hemodynamics. arXiv preprint arXiv:2501.09980 (2025).
- 319 [19] Ding, W., Ji, K., Castro, S., Luo, Y., Roi, D., Yap, C.H.: Two-Stage Generative Model for
 320 Intracranial Aneurysm Meshes with Morphological Marker Conditioning. Medical Image
 321 Computing and Computer Assisted Intervention – MICCAI 2025, Lecture Notes in Computer
 322 Science **15969**, 595–604 (2025).
- 323 [20] Luo, Y., Sesija, D., Wang, F., Wu, Y., Ding, W., Huang, J., et al.: Explicit Differentiable Slicing
 324 and Global Deformation for Cardiac Mesh Reconstruction. arXiv preprint arXiv:2409.02070v2
 325 (2024).
- 326 [21] Juchler, N., Schilling, S., Bijlenga, P., Kurtcuoglu, V., Hirsch, S.: AneuX: Shape Trumps Size
 327 — Image-Based Morphological Analysis Reveals that the 3D Shape Discriminates Intracranial
 328 Aneurysm Disease Status Better than Aneurysm Size. Frontiers in Neurology **13**, 809391 (2022).
- 329 [22] Ding, W.: AneuG-Flow: Dataset and mesh generation code for intracranial aneurysm flow
 330 prediction. GitHub repository, https://github.com/WenHaoDing/AneG_Flow (2025).
- 331 [23] Weston, M.E., Barker, A.R., Tomlinson, O.W., Coombes, J.S., Bailey, T.G., Bond, B.: Middle
 332 Cerebral Artery Blood Velocity and End-Tidal Carbon Dioxide Responses to Moderate Intensity
 333 Cycling in Children, Adolescents, and Adults. Journal of Applied Physiology **137**(5), 1117–1129
 334 (2024).
- 335 [24] Chnafa, C., Brina, O., Pereira, V.M., Steinman, D.A.: Better Than Nothing: A Rational
 336 Approach for Minimizing the Impact of Outflow Strategy on Cerebrovascular Simulations.
 337 American Journal of Neuroradiology **39**(2), 337–343 (2018).
- 338 [25] Saalfeld, S., Voß, S., Beuing, O., Preim, B., Berg, P.: Flow-Splitting-Based Computation of
 339 Outlet Boundary Conditions for Improved Cerebrovascular Simulation in Multiple Intracranial
 340 Aneurysms. International Journal of Computer Assisted Radiology and Surgery **14**(10), 1805–
 341 1813 (2019).
- 342 [26] Chnafa, C., Bouillot, P., Brina, O., Delattre, B.M.A., Vargas, M.I., Lovblad, K.O., Pereira, V.M.,
 343 Steinman, D.A.: Vessel calibre and flow splitting relationships at the internal carotid artery
 344 terminal bifurcation. *Physiological Measurement* **38**(11), 2044–2057 (2017).
- 345 [27] Ford, M.D., Alperin, N., Lee, S.H., Holdsworth, D.W., Steinman, D.A.: Characterization of vol-
 346 umetric flow rate waveforms in the normal internal carotid and vertebral arteries. *Physiological*
 347 *Measurement* **26**(4), 477–488 (2005).
- 348 [28] Qi, C.R., Yi, L., Su, H., Guibas, L.J.: PointNet++: Deep Hierarchical Feature Learning on Point
 349 Sets in a Metric Space. arXiv preprint arXiv:1706.02413 (2017).
- 350 [29] Tan, Q., Gao, L., Lai, Y.-K., Xia, S.: Variational Autoencoders for Deforming 3D Mesh Models.
 351 In: Proceedings of the IEEE Conference on Computer Vision and Pattern Recognition (CVPR),
 352 pp. 5841–5850 (2018).
- 353 [30] Trenti, C., Ziegler, M., Bjarnegård, N., et al.: Wall shear stress and relative residence time
 354 as potential risk factors for abdominal aortic aneurysms in males: a 4D flow cardiovascular
 355 magnetic resonance case-control study. *Journal of Cardiovascular Magnetic Resonance* **24**, 18
 356 (2022). 10.1186/s12968-022-00848-2

357 **NeurIPS Paper Checklist**

358 The checklist is designed to encourage best practices for responsible machine learning research,
359 addressing issues of reproducibility, transparency, research ethics, and societal impact. Do not remove
360 the checklist: **The papers not including the checklist will be desk rejected.** The checklist should
361 follow the references and follow the (optional) supplemental material. The checklist does NOT count
362 towards the page limit.

363 Please read the checklist guidelines carefully for information on how to answer these questions. For
364 each question in the checklist:

- 365 • You should answer [Yes] , [No] , or [NA] .
366 • [NA] means either that the question is Not Applicable for that particular paper or the
367 relevant information is Not Available.
368 • Please provide a short (1–2 sentence) justification right after your answer (even for NA).

369 **The checklist answers are an integral part of your paper submission.** They are visible to the
370 reviewers, area chairs, senior area chairs, and ethics reviewers. You will be asked to also include it
371 (after eventual revisions) with the final version of your paper, and its final version will be published
372 with the paper.

373 The reviewers of your paper will be asked to use the checklist as one of the factors in their evaluation.
374 While "[Yes]" is generally preferable to "[No]", it is perfectly acceptable to answer "[No]" provided a
375 proper justification is given (e.g., "error bars are not reported because it would be too computationally
376 expensive" or "we were unable to find the license for the dataset we used"). In general, answering
377 "[No]" or "[NA]" is not grounds for rejection. While the questions are phrased in a binary way, we
378 acknowledge that the true answer is often more nuanced, so please just use your best judgment and
379 write a justification to elaborate. All supporting evidence can appear either in the main paper or the
380 supplemental material, provided in appendix. If you answer [Yes] to a question, in the justification
381 please point to the section(s) where related material for the question can be found.

382 **IMPORTANT**, please:

- 383 • **Delete this instruction block, but keep the section heading "NeurIPS Paper Checklist",**
384 • **Keep the checklist subsection headings, questions/answers and guidelines below.**
385 • **Do not modify the questions and only use the provided macros for your answers.**

386 **1. Claims**

387 Question: Do the main claims made in the abstract and introduction accurately reflect the
388 paper's contributions and scope?

389 Answer: [Yes]

390 Justification: Main contributions are covered in the introduction.

391 Guidelines:

- 392 • The answer NA means that the abstract and introduction do not include the claims
393 made in the paper.
394 • The abstract and/or introduction should clearly state the claims made, including the
395 contributions made in the paper and important assumptions and limitations. A No or
396 NA answer to this question will not be perceived well by the reviewers.
397 • The claims made should match theoretical and experimental results, and reflect how
398 much the results can be expected to generalize to other settings.
399 • It is fine to include aspirational goals as motivation as long as it is clear that these goals
400 are not attained by the paper.

401 **2. Limitations**

402 Question: Does the paper discuss the limitations of the work performed by the authors?

403 Answer: [Yes]

404 Justification: Limitations are discussed in Section 3.4.

405 Guidelines:

- 406 • The answer NA means that the paper has no limitation while the answer No means that
407 the paper has limitations, but those are not discussed in the paper.
- 408 • The authors are encouraged to create a separate "Limitations" section in their paper.
- 409 • The paper should point out any strong assumptions and how robust the results are to
410 violations of these assumptions (e.g., independence assumptions, noiseless settings,
411 model well-specification, asymptotic approximations only holding locally). The authors
412 should reflect on how these assumptions might be violated in practice and what the
413 implications would be.
- 414 • The authors should reflect on the scope of the claims made, e.g., if the approach was
415 only tested on a few datasets or with a few runs. In general, empirical results often
416 depend on implicit assumptions, which should be articulated.
- 417 • The authors should reflect on the factors that influence the performance of the approach.
418 For example, a facial recognition algorithm may perform poorly when image resolution
419 is low or images are taken in low lighting. Or a speech-to-text system might not be
420 used reliably to provide closed captions for online lectures because it fails to handle
421 technical jargon.
- 422 • The authors should discuss the computational efficiency of the proposed algorithms
423 and how they scale with dataset size.
- 424 • If applicable, the authors should discuss possible limitations of their approach to
425 address problems of privacy and fairness.
- 426 • While the authors might fear that complete honesty about limitations might be used by
427 reviewers as grounds for rejection, a worse outcome might be that reviewers discover
428 limitations that aren't acknowledged in the paper. The authors should use their best
429 judgment and recognize that individual actions in favor of transparency play an impor-
430 tant role in developing norms that preserve the integrity of the community. Reviewers
431 will be specifically instructed to not penalize honesty concerning limitations.

432 **3. Theory assumptions and proofs**

433 Question: For each theoretical result, does the paper provide the full set of assumptions and
434 a complete (and correct) proof?

435 Answer: [Yes]

436 Justification: Full assumptions are covered in Section 2.3. Mesh and time-step convergence
437 analyses are covered in the supplementary material.

438 Guidelines:

- 439 • The answer NA means that the paper does not include theoretical results.
- 440 • All the theorems, formulas, and proofs in the paper should be numbered and cross-
441 referenced.
- 442 • All assumptions should be clearly stated or referenced in the statement of any theorems.
- 443 • The proofs can either appear in the main paper or the supplemental material, but if
444 they appear in the supplemental material, the authors are encouraged to provide a short
445 proof sketch to provide intuition.
- 446 • Inversely, any informal proof provided in the core of the paper should be complemented
447 by formal proofs provided in appendix or supplemental material.
- 448 • Theorems and Lemmas that the proof relies upon should be properly referenced.

449 **4. Experimental result reproducibility**

450 Question: Does the paper fully disclose all the information needed to reproduce the main ex-
451 perimental results of the paper to the extent that it affects the main claims and/or conclusions
452 of the paper (regardless of whether the code and data are provided or not)?

453 Answer: [No]

454 Justification: We do not describe all details of the network design. However, we do provide
455 them in the codes.

456 Guidelines:

- 457 • The answer NA means that the paper does not include experiments.

- 458 • If the paper includes experiments, a No answer to this question will not be perceived
 459 well by the reviewers: Making the paper reproducible is important, regardless of
 460 whether the code and data are provided or not.
 461 • If the contribution is a dataset and/or model, the authors should describe the steps taken
 462 to make their results reproducible or verifiable.
 463 • Depending on the contribution, reproducibility can be accomplished in various ways.
 464 For example, if the contribution is a novel architecture, describing the architecture fully
 465 might suffice, or if the contribution is a specific model and empirical evaluation, it may
 466 be necessary to either make it possible for others to replicate the model with the same
 467 dataset, or provide access to the model. In general, releasing code and data is often
 468 one good way to accomplish this, but reproducibility can also be provided via detailed
 469 instructions for how to replicate the results, access to a hosted model (e.g., in the case
 470 of a large language model), releasing of a model checkpoint, or other means that are
 471 appropriate to the research performed.
 472 • While NeurIPS does not require releasing code, the conference does require all submissions
 473 to provide some reasonable avenue for reproducibility, which may depend on the
 474 nature of the contribution. For example
 475 (a) If the contribution is primarily a new algorithm, the paper should make it clear how
 476 to reproduce that algorithm.
 477 (b) If the contribution is primarily a new model architecture, the paper should describe
 478 the architecture clearly and fully.
 479 (c) If the contribution is a new model (e.g., a large language model), then there should
 480 either be a way to access this model for reproducing the results or a way to reproduce
 481 the model (e.g., with an open-source dataset or instructions for how to construct
 482 the dataset).
 483 (d) We recognize that reproducibility may be tricky in some cases, in which case
 484 authors are welcome to describe the particular way they provide for reproducibility.
 485 In the case of closed-source models, it may be that access to the model is limited in
 486 some way (e.g., to registered users), but it should be possible for other researchers
 487 to have some path to reproducing or verifying the results.

488 5. Open access to data and code

489 Question: Does the paper provide open access to the data and code, with sufficient instruc-
 490 tions to faithfully reproduce the main experimental results, as described in supplemental
 491 material?

492 Answer: [Yes]

493 Justification: Links can be found in Section 3.3.

494 Guidelines:

- 495 • The answer NA means that paper does not include experiments requiring code.
 496 • Please see the NeurIPS code and data submission guidelines (<https://nips.cc/public/guides/CodeSubmissionPolicy>) for more details.
 497 • While we encourage the release of code and data, we understand that this might not be
 498 possible, so “No” is an acceptable answer. Papers cannot be rejected simply for not
 499 including code, unless this is central to the contribution (e.g., for a new open-source
 500 benchmark).
 501 • The instructions should contain the exact command and environment needed to run to
 502 reproduce the results. See the NeurIPS code and data submission guidelines (<https://nips.cc/public/guides/CodeSubmissionPolicy>) for more details.
 503 • The authors should provide instructions on data access and preparation, including how
 504 to access the raw data, preprocessed data, intermediate data, and generated data, etc.
 505 • The authors should provide scripts to reproduce all experimental results for the new
 506 proposed method and baselines. If only a subset of experiments are reproducible, they
 507 should state which ones are omitted from the script and why.
 508 • At submission time, to preserve anonymity, the authors should release anonymized
 509 versions (if applicable).

- 512 • Providing as much information as possible in supplemental material (appended to the
513 paper) is recommended, but including URLs to data and code is permitted.

514 **6. Experimental setting/details**

515 Question: Does the paper specify all the training and test details (e.g., data splits, hyper-
516 parameters, how they were chosen, type of optimizer, etc.) necessary to understand the
517 results?

518 Answer: [No]

519 Justification: We do not mention all details of the training. However, we provide them in the
520 codes.

521 Guidelines:

- 522 • The answer NA means that the paper does not include experiments.
523 • The experimental setting should be presented in the core of the paper to a level of detail
524 that is necessary to appreciate the results and make sense of them.
525 • The full details can be provided either with the code, in appendix, or as supplemental
526 material.

527 **7. Experiment statistical significance**

528 Question: Does the paper report error bars suitably and correctly defined or other appropriate
529 information about the statistical significance of the experiments?

530 Answer: [NA]

531 Justification: Our dataset is simulated with synthetic geometries, we therefore do not have
532 statistical significance of the experiments.

533 Guidelines:

- 534 • The answer NA means that the paper does not include experiments.
535 • The authors should answer "Yes" if the results are accompanied by error bars, confi-
536 dence intervals, or statistical significance tests, at least for the experiments that support
537 the main claims of the paper.
538 • The factors of variability that the error bars are capturing should be clearly stated (for
539 example, train/test split, initialization, random drawing of some parameter, or overall
540 run with given experimental conditions).
541 • The method for calculating the error bars should be explained (closed form formula,
542 call to a library function, bootstrap, etc.)
543 • The assumptions made should be given (e.g., Normally distributed errors).
544 • It should be clear whether the error bar is the standard deviation or the standard error
545 of the mean.
546 • It is OK to report 1-sigma error bars, but one should state it. The authors should
547 preferably report a 2-sigma error bar than state that they have a 96% CI, if the hypothesis
548 of Normality of errors is not verified.
549 • For asymmetric distributions, the authors should be careful not to show in tables or
550 figures symmetric error bars that would yield results that are out of range (e.g. negative
551 error rates).
552 • If error bars are reported in tables or plots, The authors should explain in the text how
553 they were calculated and reference the corresponding figures or tables in the text.

554 **8. Experiments compute resources**

555 Question: For each experiment, does the paper provide sufficient information on the com-
556 puter resources (type of compute workers, memory, time of execution) needed to reproduce
557 the experiments?

558 Answer: [Yes]

559 Justification: Related information are reported in Section 2.4.

560 Guidelines:

- 561 • The answer NA means that the paper does not include experiments.

- 562 • The paper should indicate the type of compute workers CPU or GPU, internal cluster,
563 or cloud provider, including relevant memory and storage.
564 • The paper should provide the amount of compute required for each of the individual
565 experimental runs as well as estimate the total compute.
566 • The paper should disclose whether the full research project required more compute
567 than the experiments reported in the paper (e.g., preliminary or failed experiments that
568 didn't make it into the paper).

569 **9. Code of ethics**

570 Question: Does the research conducted in the paper conform, in every respect, with the
571 NeurIPS Code of Ethics <https://neurips.cc/public/EthicsGuidelines>?

572 Answer: [Yes]

573 Justification: [NA]

574 Guidelines:

- 575 • The answer NA means that the authors have not reviewed the NeurIPS Code of Ethics.
576 • If the authors answer No, they should explain the special circumstances that require a
577 deviation from the Code of Ethics.
578 • The authors should make sure to preserve anonymity (e.g., if there is a special consid-
579 eration due to laws or regulations in their jurisdiction).

580 **10. Broader impacts**

581 Question: Does the paper discuss both potential positive societal impacts and negative
582 societal impacts of the work performed?

583 Answer: [NA]

584 Justification: [NA]

585 Guidelines:

- 586 • The answer NA means that there is no societal impact of the work performed.
587 • If the authors answer NA or No, they should explain why their work has no societal
588 impact or why the paper does not address societal impact.
589 • Examples of negative societal impacts include potential malicious or unintended uses
590 (e.g., disinformation, generating fake profiles, surveillance), fairness considerations
591 (e.g., deployment of technologies that could make decisions that unfairly impact specific
592 groups), privacy considerations, and security considerations.
593 • The conference expects that many papers will be foundational research and not tied
594 to particular applications, let alone deployments. However, if there is a direct path to
595 any negative applications, the authors should point it out. For example, it is legitimate
596 to point out that an improvement in the quality of generative models could be used to
597 generate deepfakes for disinformation. On the other hand, it is not needed to point out
598 that a generic algorithm for optimizing neural networks could enable people to train
599 models that generate Deepfakes faster.
600 • The authors should consider possible harms that could arise when the technology is
601 being used as intended and functioning correctly, harms that could arise when the
602 technology is being used as intended but gives incorrect results, and harms following
603 from (intentional or unintentional) misuse of the technology.
604 • If there are negative societal impacts, the authors could also discuss possible mitigation
605 strategies (e.g., gated release of models, providing defenses in addition to attacks,
606 mechanisms for monitoring misuse, mechanisms to monitor how a system learns from
607 feedback over time, improving the efficiency and accessibility of ML).

608 **11. Safeguards**

609 Question: Does the paper describe safeguards that have been put in place for responsible
610 release of data or models that have a high risk for misuse (e.g., pretrained language models,
611 image generators, or scraped datasets)?

612 Answer: [NA]

613 Justification: Not applicable.

614 Guidelines:

- 615 • The answer NA means that the paper poses no such risks.
- 616 • Released models that have a high risk for misuse or dual-use should be released with
- 617 necessary safeguards to allow for controlled use of the model, for example by requiring
- 618 that users adhere to usage guidelines or restrictions to access the model or implementing
- 619 safety filters.
- 620 • Datasets that have been scraped from the Internet could pose safety risks. The authors
- 621 should describe how they avoided releasing unsafe images.
- 622 • We recognize that providing effective safeguards is challenging, and many papers do
- 623 not require this, but we encourage authors to take this into account and make a best
- 624 faith effort.

625 **12. Licenses for existing assets**

626 Question: Are the creators or original owners of assets (e.g., code, data, models), used in

627 the paper, properly credited and are the license and terms of use explicitly mentioned and

628 properly respected?

629 Answer: [NA]

630 Justification: Not applicable.

631 Guidelines:

- 632 • The answer NA means that the paper does not use existing assets.
- 633 • The authors should cite the original paper that produced the code package or dataset.
- 634 • The authors should state which version of the asset is used and, if possible, include a
- 635 URL.
- 636 • The name of the license (e.g., CC-BY 4.0) should be included for each asset.
- 637 • For scraped data from a particular source (e.g., website), the copyright and terms of
- 638 service of that source should be provided.
- 639 • If assets are released, the license, copyright information, and terms of use in the
- 640 package should be provided. For popular datasets, paperswithcode.com/datasets
- 641 has curated licenses for some datasets. Their licensing guide can help determine the
- 642 license of a dataset.
- 643 • For existing datasets that are re-packaged, both the original license and the license of
- 644 the derived asset (if it has changed) should be provided.
- 645 • If this information is not available online, the authors are encouraged to reach out to
- 646 the asset's creators.

647 **13. New assets**

648 Question: Are new assets introduced in the paper well documented and is the documentation

649 provided alongside the assets?

650 Answer: [NA]

651 Justification: [NA]

652 Guidelines:

- 653 • The answer NA means that the paper does not release new assets.
- 654 • Researchers should communicate the details of the dataset/code/model as part of their
- 655 submissions via structured templates. This includes details about training, license,
- 656 limitations, etc.
- 657 • The paper should discuss whether and how consent was obtained from people whose
- 658 asset is used.
- 659 • At submission time, remember to anonymize your assets (if applicable). You can either
- 660 create an anonymized URL or include an anonymized zip file.

661 **14. Crowdsourcing and research with human subjects**

662 Question: For crowdsourcing experiments and research with human subjects, does the paper

663 include the full text of instructions given to participants and screenshots, if applicable, as

664 well as details about compensation (if any)?

665 Answer: [NA]

666 Justification: Not applicable.

667 Guidelines:

- The answer NA means that the paper does not involve crowdsourcing nor research with human subjects.
- Including this information in the supplemental material is fine, but if the main contribution of the paper involves human subjects, then as much detail as possible should be included in the main paper.
- According to the NeurIPS Code of Ethics, workers involved in data collection, curation, or other labor should be paid at least the minimum wage in the country of the data collector.

676 **15. Institutional review board (IRB) approvals or equivalent for research with human
677 subjects**

678 Question: Does the paper describe potential risks incurred by study participants, whether
679 such risks were disclosed to the subjects, and whether Institutional Review Board (IRB)
680 approvals (or an equivalent approval/review based on the requirements of your country or
681 institution) were obtained?

682 Answer: [NA]

683 Justification: Not applicable.

684 Guidelines:

- The answer NA means that the paper does not involve crowdsourcing nor research with human subjects.
- Depending on the country in which research is conducted, IRB approval (or equivalent) may be required for any human subjects research. If you obtained IRB approval, you should clearly state this in the paper.
- We recognize that the procedures for this may vary significantly between institutions and locations, and we expect authors to adhere to the NeurIPS Code of Ethics and the guidelines for their institution.
- For initial submissions, do not include any information that would break anonymity (if applicable), such as the institution conducting the review.

695 **16. Declaration of LLM usage**

696 Question: Does the paper describe the usage of LLMs if it is an important, original, or
697 non-standard component of the core methods in this research? Note that if the LLM is used
698 only for writing, editing, or formatting purposes and does not impact the core methodology,
699 scientific rigorosity, or originality of the research, declaration is not required.

700 Answer: [NA]

701 Justification: LLM is used for minor grammar checking, but not for any methodology parts.

702 Guidelines:

- The answer NA means that the core method development in this research does not involve LLMs as any important, original, or non-standard components.
- Please refer to our LLM policy (<https://neurips.cc/Conferences/2025/LLM>) for what should or should not be described.